Electrokinetic Assembly of Selenium and Silver Nanowires into Macroscopic Fibers

Michael C. P. Wang,[†] Xin Zhang,[†] Elham Majidi,[†] Kevin Nedelec,[‡,†] and Byron D. Gates[†,*]

Department of Chemistry, Simon Fraser University, 8888 University Drive, Burnaby, BC, V5A 1S6, Canada. [†]Department of Chemistry and 4D LABS, Simon Fraser University. [‡]Research assistant visiting SFU from Département Science des Matériaux, Polytech'Nantes, Université de Nantes, Rue Christian Pauc, BP 50609, 44306 Nantes Cedex 3, France.

ABSTRACT Solution-phase synthesized nanowires with high aspect ratios can be a challenge to assemble into desired structures. As synthesized, these nanostructures readily bend and entangle with each other to form larger aggregates. This manuscript reports a general procedure for directing the assembly of semiconducting and metallic nanowires into fibers that can easily span distances >1 cm. Dispersions of these nanostructures in a low dielectric solution are organized by electrokinetic techniques into fibers that can be isolated from solution. Theoretical studies suggest that the assembled fibers adopt an orientation along electric field lines in the solution. The number of assembled fibers is a function of the duration of the assembly process, the magnitude of the electric potential, and the initial concentration of nanowires dispersed in solution. These findings offer a general method for the assembly of nanowires into macroscopic fibers of tunable dimensions. Fibers of selenium nanowires isolated from solution can reversibly bend in response to a source of electrostatic charges positioned in close proximity to the free-standing fiber. These flexible selenium fibers also exhibit a photoconductive response when illuminated with white light.

KEYWORDS: assembly · metal nanowires · semiconducting nanowires · electrokinetics · fibers

Synthetic techniques can produce nanostructures with a diverse set of shapes and an equally diverse range of dimensions and compositions.[1−7] Harnessing these materials for their nanoscale properties requires the ability to handle and manipulate the materials. Although much attention has been given to the manipulation of many nanoscale materials,[8−17] some structures have received relatively little attention. One type of structure that requires further development of techniques for their assembly are solution-phase synthesized nanowires.[18] Some attention has been given to the assembly of carbon nanotubes, another highly anisotropic nanostructure. These nanotubes can be assembled during or after synthesis.[19−23] One lesson to learn from the previous work on manipulating nanoscale materials is the importance of developing techniques that can be appropriately scaled to assemble nanostructures in parallel for a range of concentrations. The challenge is to extend this concept to nanowires that require solution-based techniques for manipulation. Our goal is to develop appropriate techniques to direct nanowires into assemblies that span over large distances (>5 cm) within a few minutes for further manipulation and utilization of these materials.

The challenge of directing the assembly of synthetic nanowires increases as the length (or aspect ratio) of these structures also increases. This correlation is attributed to an increased flexibility and fragility of these nanostructures.[24] Nanowires with a small aspect ratio are relatively stiff structures, but nanowires with high aspect ratios (*e.g.*, 1:1000, diameter/length) are flexible and easily entwined with other nanowires (Supporting Information, Figure S1). This process of self-entanglement can be avoided by dilution of the nanowire suspensions. However, assembly of nanowires one-by-one or in low quantities is inefficient and impractical for many applications. A number of approaches can be implemented to assemble nanowires.[18] Ideally, the technique for directing the assembly of nanowires would be independent of the material composition, scalable over multiple lengths, and applicable to a wide range of nanowire concentrations.

Electrokinetics is a promising approach to manipulating nanowires. Directing the assembly of nanostructures within an electric field has a number of benefits and limitations. Materials can assemble based on polarization of the material and the interactions of charge within an applied electric field.[8,22,25−32] The electric field lines direct the assembly of the materials and can, therefore, be used to assemble multiple nanostructures in a parallel process.

*Address correspondence to bgates@sfu.ca.

Received for review December 29, 2009 and accepted March 24, 2010.

Published online April 15, 2010.
10.1021/nn901923z

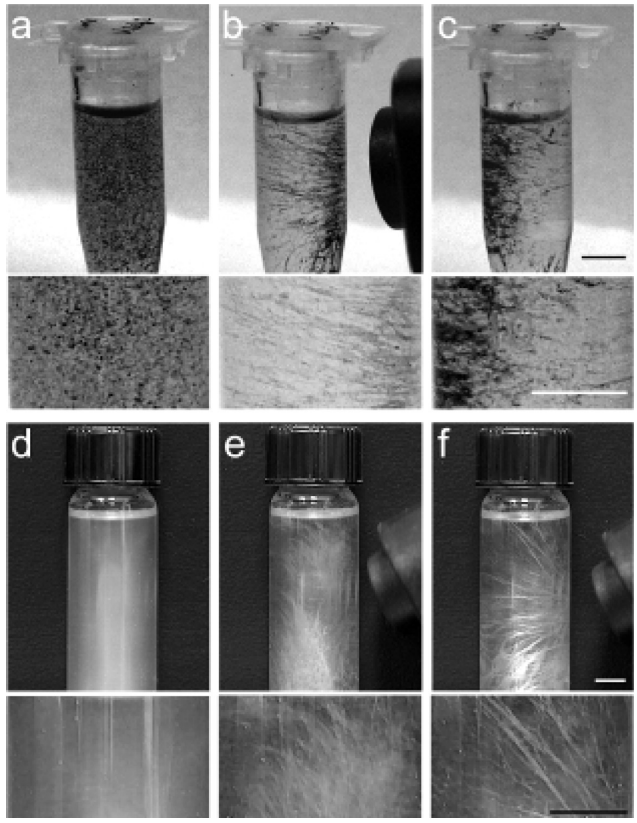

Figure 1. Optical images show that dispersions of (a) selenium and (d) silver nanowires in hexanes align with electric field lines created after the exterior of the plastic or glass vial is exposed to charged ions generated from a hand-held Zerostat antistatic gun. Selenium nanowires (b) collect into fibers extending from the region nearest to the source of charge when positive ions are generated and (c) repel from this interface upon generation of negative ions. The opposite response is observed for silver nanowires when (e) positive and (f) negative ions are generated by the Zerostat antistatic gun. All scale bars are 0.5 cm.

In addition, the process can be reversible if electrochemical degradation of the sample is avoided during the assembly process. This ability to reconfigure the assembled nanostructures can be useful for optimizing their positions by cycling between assembly and dispersion processes. The field lines can also be directed over distances much larger than the largest dimension of the nanostructures. These properties have been used to assemble nanowires of metals, semiconductors, and dielectric materials over distances of a few micrometers,[27−30] but for highly anisotropic nanostructures, only carbon nanotubes have been assembled over larger distances through the use of electrokinetics.[20,23] We demonstrate herein the ability to use electrokinetics to direct the assembly of solution-phase synthesized nanowires over large distances (>5 cm).

RESULTS AND DISCUSSION

Elecrokinetic assembly of nanostructures requires a dispersion of either polarizable or charged materials.[33] Assembly proceeds by either dielectrophoresis or electrophoresis.[33,34] To design a general system for assembly, we chose a low dielectric solution in which the nanostructures would be suspended. This type of solution will maximize the response of our system to applied electric fields. The first systems we tested were the response of suspensions of selenium and silver nanowires (detailed syntheses of the nanowires are described in Materials and Methods) to static electric fields established by externally applied charges. A number of methods can generate charge to create this external electric field, such as Van de Graaf generators, Tesla coils, and piezoelectric charge generators. The later method ionizes air molecules and is often used to dispel electrostatic charge accumulated within dry chemical powders.[35] We use a commercially available Zerostat antistatic gun to apply charge to the exterior of vessels containing dispersions of nanowires (Figure 1). The initial dispersion of ~50 μm long selenium nanowires, which have a zeta potential of −54.3 ± 2.3 mV, are attracted to the wall of the vessel when positive ions are generated[36] and repelled when negative ions are subsequently produced by the Zerostat antistatic gun. This process is reversible and can be repeated multiple times. Dispersions of ~10 μm long silver nanowires with a zeta potential of 43.3 ± 5.0 mV exhibit an equal and opposite response to the charge accumulated on the vessel; these metal nanowires are repelled by positive charge accumulation and attracted to the side of the vessel with a subsequent generation of negative ions. In both systems, the assembled nanowires appear to align with electric field lines extending from the charge accumulated on the exterior of the container to the nearest ground, such as the table top.

The solvent plays an important role in the electrokinetic assembly of the nanowires into macroscopic fibers. Solvent properties that influence the dispersion of nanowires within a solvent also influence their assembly into fibers. These properties include dielectric constant of the medium, viscosity of the medium, polarity of the medium and of the suspended material, and zeta potential of the dispersed nanostructures.[31,32] It is anticipated that viscosity plays a minor role in the ability to form fibers from dispersed nanowires. We screened a number of solvents with similar viscosities. These solvents had very different solvent polarities and dielectric constants. Our studies revealed that dielectric constant of the solvent played a dominate role in determining whether dispersed nanowires would successfully assemble into a visible macroscopic fiber (Table 1). From the low dielectric solvents that we screened, hexanes was chosen as the preferred solvent for assembly of the fiber-like structures. This choice was dictated by a combination of macroscopic fiber stability in each solvent and boiling point of the solvent.

Selenium and alkanethiol-modified silver nanowires dispersed within low dielectric solvents (*i.e.*, dielectric constants ≤ 4.34) could assemble into macroscopic fibers under an applied electric field. A similar method of

TABLE 1. Solvent Dependence for the Assembly of Nanowires into Macroscopic Fibers[a,37,38]

solvent	ε_r	P'	forms fiber
hexanes	1.89	0	yes
hexafluorobenzene	2.02	0	yes
1,4-dioxane	2.2	4.8	yes
carbon tetrachloride	2.23	1.6	yes
toluene	2.37	2.4	yes
diethyl ether	4.34	2.8	yes
chloroform	4.8	4.1	no
tetrahydrofuran	7.6	4	no
ethanol	25.3	5.2	no
acetonitrile	37.5	5.8	no

[a]Abbreviations: ε_r = dielectric constant and P' = solvent polarity.

assembly was reported by Kamat *et al.*[20] Kamat introduced extrinsic charges onto the surfaces of their materials through the addition of an ionic surfactant to polarize their material under applied electric fields. In comparison to our study, Kamat *et al.* were able to assemble their material into linear bundles along electric field lines in a relatively high dielectric constant solvent. In our system, both selenium and silver nanowires were assembled into macroscopic fibers without the addition of charged surfactants. The assembly of nanowires in our system relies on a combination of material polarization and dispersion in the solvent. Low dielectric constant solvents were required in our method of nanowire assembly. The insulating properties of these solvents prevented loss of charge or screening of polarization from the nanowires within the electrostatic field.

Fine tuning the response of the assembled system requires the use of a variable power supply to control the strength of the applied electric field. The distance covered by the assembled nanowires and the density of the nanowires collected within the electric field lines should scale with the strength of the applied field. The type of power supply necessary to direct the assembly of nanostructures within a low dielectric solution can be estimated from the electrostatic potential used in the previous study (*e.g.*, 2−5 kV for a Zerostat antistatic gun). Electrodes from a high voltage DC power supply connected to opposing sides of a glass vial can establish electric field lines within the container for directing the organization of nanostructures. The nanowires assemble into macroscale fibers extending from the walls of the container. These fibers span the diameter of the vial between the two external electrodes (Figure 2). Increasing the applied field strength increases both the length and the quantity of assembled fibers. Lengths of the fibers are limited by the distance between the two electrodes or the distance to a second, more efficient source of ground (Supporting Information, Figure S2). To achieve larger assemblies, the systems need to be isolated from unwanted grounding sources.

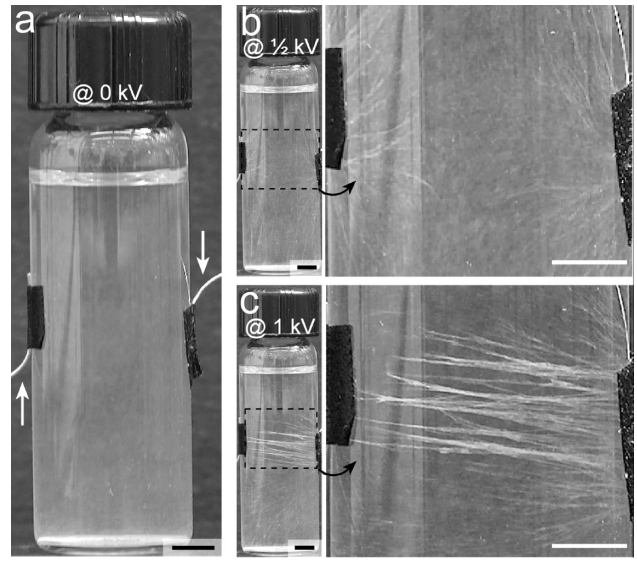

Figure 2. Optical images of silver nanowires assembled into fibers by electrokinetic processes. (a) Silver nanowires dispersed in hexanes align with electric field lines (b,c) created using an external power supply. Electrodes from this power supply are in contact with opposite sides of the glass vial at the positions indicated by the white arrows in (a). Increasing the electric field strength (0.33 MV/m in b, and 0.67 MV/m in c) increased the density and length of the fibers assembled between the two electrodes. Similar results were also observed for the assembly of selenium nanowires (Supporting Information, Figure S2). All scale bars are 0.4 cm.

There are few options to isolate a system containing high voltage field lines from external, unwanted grounding sources. One of the best electric insulators is air. A simple method for insulating our system is to suspend it in air. A number of insulating containers of either plastic or glass could be used to contain the dispersions of nanowires during the assembly process. A simple and inexpensive container is an open glass dish, such as a glass Petri dish or crystallizing dish. This setup can be easily viewed from above or from the side with minimal distortion. The new container is also convenient for assessing the dynamics of the assembling nanowires. In this configuration, the choice of electrode is important to avoid unwanted electrochemical reactions between the nanowires and the electrode. For example, although copper wires can be used to direct assembly within the solution, the nanowires and the electrodes can electrochemically react during this process. Platinum wires are the preferred choice for directing the assembly of selenium or silver nanowires. Material in solution starts to assemble into fiber-like structures extending from these electrodes as soon as a sufficient electric field is applied to the solution. These fibers will grow to lengths of ~1 cm in <30 s and continue to grow in both length and width as more nanowires accumulate along the field lines over time (Figure 3). The fibers and field lines can extend in all directions from a single working electrode. Fibers can also form between electrodes with orientations along the applied field lines (Figure 3b and Supporting Information, Figure S3).

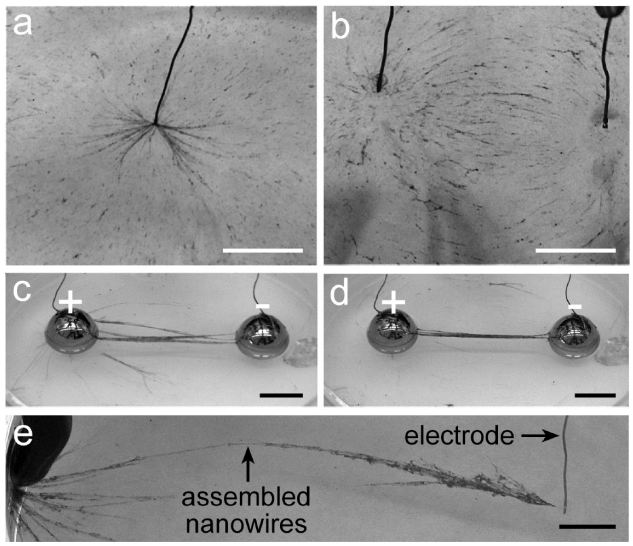

Figure 3. Selenium nanowires assemble into fibers along electric field lines generated in a solution of hexanes. Visible fibers are observed extending (a) from a single working electrode or (b) between two electrodes in close proximity. In both (a) and (b), a field of 1.7 MV/m was applied for 30 s. (c−e) Centimeter long fibers can form between the two electrodes. Increasing the field strength (*e.g.*, from 1.6 MV/m in c to 3.3 MV/m in d) drives the assembly of the nanowires into a single fiber. Scale bars in a−e are 1 cm.

Increasing the field strength concentrates the nanowires into a single fiber spanning the shortest path between the working and ground electrodes. The onset of assembly for both selenium and silver nanowires into macroscopic fibers was visually observed for field strengths >0.30 MV/m, and fibers of appreciable length (>1 cm) are seen at ~0.50 MV/m. The assembled fibers continue to gather nanowires from solution until reaching ~9 MV/m. At this field strength, fiber-like structures were observed to shuttle back and forth between the two electrodes. It is likely that these bundles of selenium or silver nanowires are carrying charge between the electrodes and may be undergoing electrochemical reactions at the electrodes. Many low dielectric solvents should be stable at this potential. Hexane, for example, has a breakdown potential of 246 MV/m.[39] It is possible that reactions at both electrodes could occur between the nanowire and the oxygen or water present in the solution. However, the source of the charge remains unclear as any structural or chemical changes to the nanowires remains below the detection limits of X-ray diffraction and X-ray photoelectron spectroscopy (Supporting Information, Figures S1 and S4). It is likely that the demonstrated method of assembly is very sensitive to small amounts of charge present within the solution.

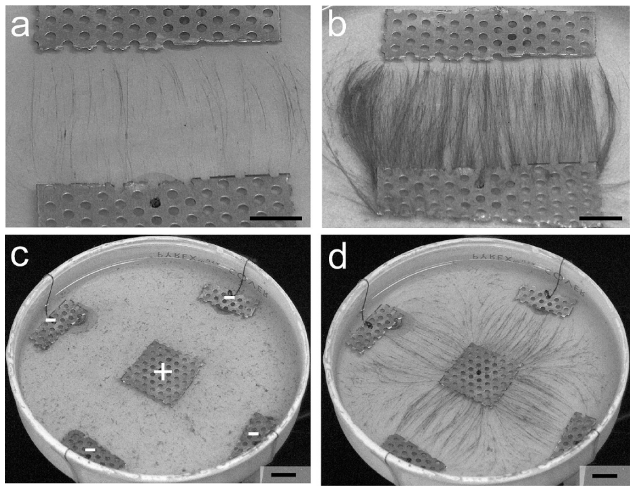

Figure 4. Optical images of selenium nanowires assembled into arrays of fibers. (a) Suspensions of nanowires (~5 μg of selenium nanowires) can be assembled between electrodes fabricated from stainless steel mesh. (b) Increasing the concentration of suspended nanowires (~120 μg) will increase the number of assembled fiber-like structures between the two opposing electrodes. (c) The geometry and relative positions of the working and ground electrodes can be used to (d) assemble nanowires (~80 μg) into fibers of a desired configuration. In both (c) and (d) electrical contact with the central electrode is made through a hole in the bottom of the glass dish. All scale bars are 1 cm and all field strengths are 2 MV/m.

To further demonstrate the versatility and scalability of the system, we pursued a number of different electrode configurations for directing the nanowires into arrays of fibers. The fibers form along electric field lines in solution, which seek the path of least resistance between the working and the ground electrodes. Parallel assembly of nanowires into multiple fibers can be achieved by increasing the area of either the working or ground electrodes (Supporting Information, Figure S5). Electrodes fabricated from a stainless steel mesh demonstrate a few important considerations in the design of these larger electrodes to create desired patterns from the assembled fibers (Figure 4). Density of fibers assembled between the mesh electrodes is nonuniform across the width of the electrodes and is mostly attributed to the periodic shape of the mesh electrode. Flat protrusions of the working electrode collect a dense array of fibers along its length. Gaps between the organized fibers correspond to the recesses at the edge of the mesh electrode. Nanowires collect primarily along the regions of the highest electric field strength, which correspond to the shortest distances between the electrodes. Therefore, density of fibers can be controlled by the periodicity of the metal protrusions extending from the working electrode. The number of assembled fibers also depends on the concentration of nanowires in solution. Density of the fibers increases proportional to increases in the nanowire concentration (Figure 4).

The open glass dishes were useful for assembling long fibers of selenium nanowires. Extending this to the assembly of silver fibers presented a larger challenge. Although these metal nanowires assembled into long fibers (>1 cm) within glass vials, in the open glass dish, the silver nanowires formed short fibers (Supporting Information, Figure S6). One of the primary reasons for our inability to form long silver fibers in the open dish was the interaction of the silver nanowires with the surfaces of the glass dish. The silver nanowires had a

positive surface charge and assembled on the negative electrode. However, the negative charge of the glass also attracted these nanowires and could be one of the reasons short fibers of silver nanowires irreversibly collected on the bottom of the glass dish. Despite our attempts to protect the glass surface with a coating of 1*H*,1*H*,2*H*,2*H*-perfluorodecyltrichlorosilane, the metal nanowires irreversibly adhered to the surfaces of the glass dish. However, the nanowires collected within the region between two electrodes did align with the direction of the applied electric field.

Electrokinetic assembly of nanowires can form very long and stable fibers. Nanowires can be assembled into fibers with lengths >7 cm that are suspended in solution (Figure 3e). These fibers are stable upon removal of the applied electric field. The suspended fibers stay in contact with the electrode and remain intact except for distortions imparted by Brownian motion and gravitational forces on these dense materials (Supporting Information, Figure S7). If the aspect ratio of the nanowires is significantly decreased, the nanostructures assembled into a very different arrangement. These shorter nanowires will also assemble within the applied electric field, but the observed assemblies are no longer simple fiber-like structures. Selenium nanowires with lengths of ~1 μm assemble into thick bundles extending from the working electrode (Figure 5). These bundles do not form the long fibers that were observed for the assemblies of 50 μm long nanowires. Higher resolution imaging is required to further understand the interactions between the 50 μm nanowires within the fiber.

A simple technique to remove the selenium fibers from solution is to lift-out the fiber by placing a solid substrate beneath the fiber and gently removing the fiber and substrate from the solution. The low surface tension of hexanes minimizes potential distortions to the fiber during a quick solvent evaporation (~1 s). Scanning electron microscopy (SEM) analysis suggests that the fibers are held together by entangled nanowires (Figures 6a,b). The nanowires interact with each other in solution through van der Waals and electrostatic forces and possibly through material polarization within the applied electric field. If the fibers of selenium nanowires were not removed from solution prior to evaporation of the bulk solvent the structure of the fiber looked very different. The nanowires within the fiber collapsed into a two-dimensional structure due to reorganization during solvent evaporation over a period of 12 h (Supporting Information, Figure S8). These structures were sheets of randomly oriented nanowires with an outline in the shape of the original fiber. The collapsed structure strongly adhered to and could not be removed from the substrate.

The free-standing selenium fibers exhibited photoconductive properties. The fiber was insulating in the absence of light (Figure 6c) but became conducting

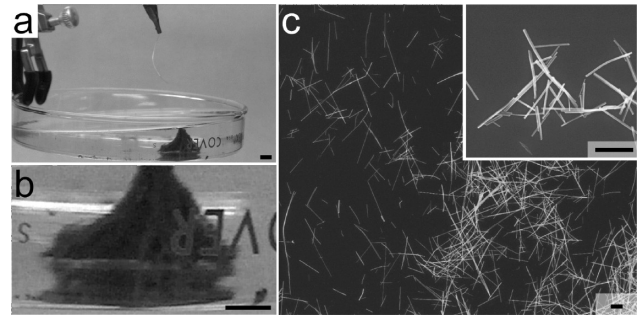

Figure 5. (a,b) Optical images of a mountainlike structure assembled by electrokinetic processes from selenium nanowires with lengths of ~1 μm. These structures grew by assembly of the short nanowires collected at the working electrode under field strengths of 5 MV/m. (c) Scanning electron microscopy (SEM) images of the original selenium nanowires with average lengths of 1.08 ± 0.44 μm. Scale bars in a and b are 0.5 cm and in c are 1 μm.

with white light illumination producing peak currents of −4.4 to 5.8 pA at −3 and 3 V, respectively. The observed current under white light illumination was noncenter symmetric, possibly due to charge accumulation on the fiber. The current passing through the selenium fiber is comparable to that reported by Liao *et al.* for a single selenium nanowire (~100 nm in diameter) over a distance of ~500 nm.[40] There are at least three possible explanations for the relatively low conductivity of our fibers. One reason is the low intensity light source used in these studies (*i.e.*, light emitting diodes) relative to that of Liao *et al.* (*i.e.*, 514 nm output from an Ar ion laser). In addition, the mobility of charge carriers decreases for nanowires with smaller diameters (our nanowires have diameters between 20 and 60 nm).[41,42] A third possible explanation for the relatively low pho-

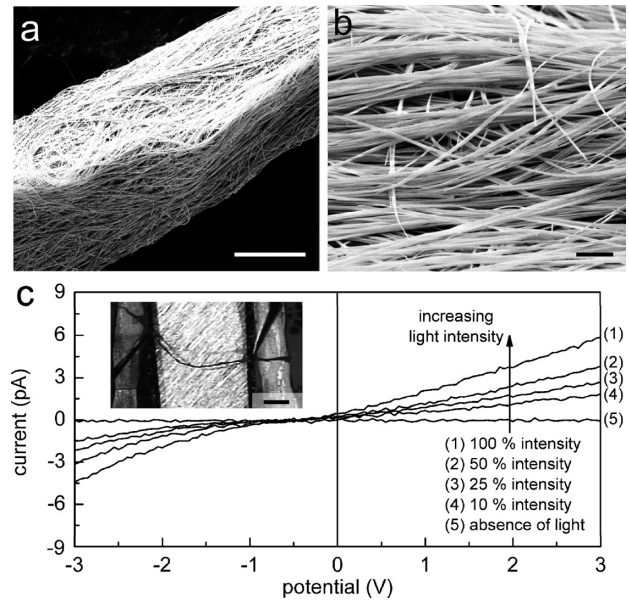

Figure 6. (a,b) Single fibers can be isolated from the solution and imaged by SEM (c) These fibers are photoconductive in response to varying intensities of white light. The inset shows an optical image of the selenium fiber on a glass substrate with a tungsten probe in contact with either end of the fiber. Scale bars are 20 μm in a, 2 μm in b, and 1 mm in c.

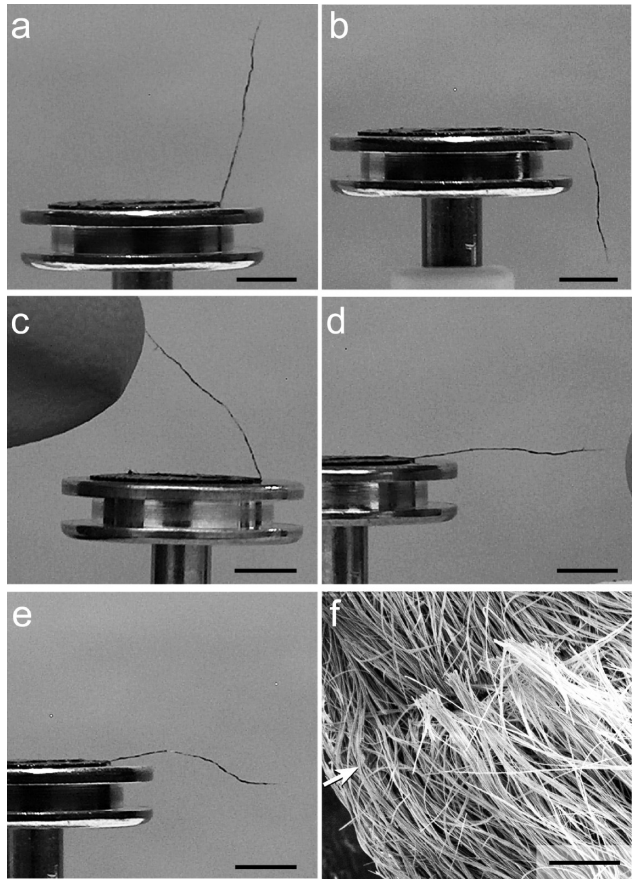

Figure 7. (a−e) Optical images of a selenium fiber partially supported on carbon tape upon an aluminum mount that is electrically insulated from ground. (a,b) This fiber is repelled by charged ions produced from a ZeroStat antistatic gun. (c,d) This same fiber is attracted to electrical ground or oppositely charged materials. (e) After bending the fiber, >200 times by steering the fiber with electrostatic charges the fiber remains intact, but (f) SEM analysis reveals fractured nanowires along the bend in the fiber (indicated by the white arrow). Scale bars in a−e are 3 mm and in f is 10 μm.

toconductivity of the assembled fibers of selenium is the increased resistance due to the long (~4 mm) and discontinuous pathway for electronic transport along the fiber.

Fibers of selenium nanowires isolated from solution exhibited the ability to reversibly bend in response to electrostatic charges brought into proximity to these fibers. A free-standing fiber bends relative to the magnitude of the electrostatic charge. One method of introducing charge onto the fibers is through the use of a ZeroStat antistatic gun. A free-standing selenium fiber deflects away from the source of the charge; the fiber can move either up or down, depending on the relative position of the external charge (Figure 7a−d). The fiber is repelled from the external charge independent of the sign of the charge (Figure 7a,b), which indicated a saturation of charge accumulated on the surfaces of the fiber. Each fiber was electrically insulated from the ground, leading to a quick accumulation of charge and a fast response (or actuation) of the fiber. These charged fibers were attracted to either an electrical ground or oppositely charged material (Figure 7c,d). The actuated fibers exhibited a high range of flexibility (reversibly bending over angles of at least 154°; see Supporting Information, Figure S9) and a moderate resistance to breaking (remaining predominately intact after bending >200 times; Figure 7e). Analysis by SEM revealed the presence of some fractured nanowires at the bend in the fiber. These fractured nanowires are predominately located near the center of the fiber (Figure 7f).

CONCLUSIONS

We have developed a technique for assembling nanowires of semiconductors and metals into macroscopic fibers directed along electric field lines when suspended in low dielectric solvents. This electrokinetic assembly is dominated by electrophoretic movement of the suspended nanowires. The assembly process is simple to implement, fast, and reversible. Multiple nanowires can be assembled in a parallel process over distances much greater than the length of individual nanowires. Anisotropic structures extending over ~7 cm assemble from dispersions of nanowires within 1 min of applying an electric potential to the solvent. These fiber-like structures can be isolated from solution or redispersed as a suspension of individual nanowires that can be assembled into another fiber. Free-standing fibers of selenium nanowires are flexible and photoconductive. Extending this technique to the assembly of individual nanowires over micrometer-scale lengths should be possible. Electrokinetic techniques are versatile and scalable for directing the assembly of solution-phase synthesized nanowires that may otherwise be difficult to organize.

MATERIALS AND METHODS

Nanowires used in the studies on electrokinetic assembly were synthesized by solution-phase techniques. Selenium nanowires were synthesized from a solid-solution-solid transformation using amorphous selenium powder. Silver nanowires are produced *via* the polyol method as discussed below.

Synthesis of Selenium Nanowires. [43] In brief, to synthesize amorphous selenium, 2.73 g (21.1 mmol) of selenious acid (H_2SeO_3, 98%; Sigma-Aldrich) was dissolved in 100 mL of 18.0 MΩ · cm water (produced *via* a Millipore water filtration system) in a 250 mL round-bottom flask. The H_2SeO_3 solution was chilled with an ice−water bath. This solution was reduced with 3 mL (61.1 mmol) of hydrazine (N_2H_4, 50−60% in water; Sigma-Aldrich), which was introduced over a 2 min period drop-by-drop into the reaction solution under magnetic stirring. After a total reaction time of 15 min, the red precipitate was collected by vacuum filtration onto a PVDF membrane (catalogue number: VVLP04700; Millipore). The filtrate was rinsed with 200 mL of ice-cold high purity water to remove residual N_2H_4. The resulting red solid was stored in a desiccator in darkness at 22 °C. Selenium nanowires were produced by sonicating for 20 s a dispersion of 1 mg of amorphous selenium powder in 1 mL of ethanol (EtOH, 95%; Commercial Alcohols) within a 1 dram glass vial. The nanowires grow over a period of 12 h while this sonicated solu-

tion was stored in darkness at 22 °C. After centrifugation at 1500 rpm for 15 min, the ethanol solution was decanted and replaced with hexanes. This solvent exchange process was repeated at least three times to remove trace amounts of ethanol. The final solution of selenium nanowires was used for the electrokinetic assembly studies.

Synthesis and Surface Modification of Silver Nanowires.[44] In the polyol synthesis of silver nanowires, 220 mg of polyvinylpyrrolidone (PVP_{55k}, M_w: 55 k; Sigma-Aldrich) dissolved in 5 mL of ethylene glycol (EG, ≥99%; Sigma-Aldrich) was heated to 120 °C with an oil bath while N_2 (g) was blown over the top of the solution at 2 mL/min to remove water vapor. When the solution reached 120 °C, 1 mL of an ethylene glycol solution containing 0.024 mg platinum(II) chloride ($PtCl_2$, 99.99+%; Aldrich) was added dropwise into the reaction mixture. The reaction proceeded under an atmosphere of N_2 (g) for 1 h before adding a solution of 50 mg of silver nitrate ($AgNO_3$, 99+%; Sigma-Aldrich) and 220 mg of PVP_{55k} dissolved in 7.5 mL of ethylene glycol. The later solution was introduced into the reaction mixture at 2 mL/min *via* a syringe pump. After the addition of this solution, the reaction temperature was increased at 1.8 °C/min to 160 °C. Upon reaching this temperature the N_2 (g) flow was removed, and the reaction flask was capped to prevent the accumulation of dust in the solution. The reaction was held at this temperature for 1 h, resulting in formation of silver nanowires. This solution of nanowires was diluted with 20 mL of acetone (Anachemia; Lab grade) and purified at least three times *via* centrifugation at 3000 rpm for 10 min, decantation of the supernatant, and redispersion in ethanol. The purified silver nanowires were coated with self-assembled monolayers of alkanethiol. A solution of 0.5 mL of 1-dodecanethiol (≥98%; Aldrich) and 1 mL of purified silver nanowires in acetone contained within a 2 mL centrifuge tube was vortexed overnight. Excess alkanethiol is removed by purification of the nanowires by at least three processes of centrifuging, decanting, and washing the modified nanowires with hexanes (≥98.5%; Anachemia).

Materials Characterization Techniques. All optical images were taken with an HP Photosmart 945 digital camera and all color images in the main body of the manuscript were altered to gray scale using Adobe Photoshop CS3 Extended software. Scanning electron microscopy (SEM) images and energy-dispersive X-ray spectroscopy (EDS) data were acquired with Strata DB235 FESEM operating at 5 kV. Samples for SEM analysis were prepared by either drop-casting a solution of nanowires or otherwise positioning the sample of interest onto a 1 cm^2 piece of silicon wafer. Bright field transmission electron microscopy (TEM) images were obtained with a Tecnai G^2 STEM operating at 200 kV. These TEM samples were prepared by drop-casting or dip-coating solutions of nanowires onto a 300 mesh copper grid coated with Formvar/carbon (catalogue number: FCF300_CU_50; Cedarlane Laboratories Limited). Average dimensions of the nanowires were calculated from more than 100 measurements obtained on different nanowires. X-ray diffraction (XRD) patterns were acquired with a Rigaku diffractometer using Cu Kα radiation. X-ray photoelectron spectra were obtained using a Kratos Analytical Axis ULTRA spectrometer containing a DLD detector. Zeta potential measurements were acquired in ethanol using a Malvern Instruments Zetasizer Nano ZS system and disposable capillary cell (catalogue number: DTS1060C; Malvern Instruments). Three consecutive measurements were made for each sample. The reported values are the mean with the error reported as one standard deviation from the mean for a normal distribution. Conductivity measurements of selenium fibers were performed on a Cascade Microtech, Inc. M150 probe station equipped with a Leica Stereo Zoom microscope, Leica ringlight LEDs (color temperature of 5000 K), and an Aglient BI500A semiconductor device analyzer. Tungsten probes were placed in direct contact with the selenium fibers and the current collected from −3 to 3 V at 50 mV increments both in the absence of light and during illumination from the LEDs of the microscope.

Electrokinetic Assembly Techniques. Care was taken to avoid the presence of dust within the solutions containing the dispersions of nanowires. Hexanes were initially filtered through a syringe filter containing a PTFE membrane with 0.2 μm holes (catalogue number: AP-4225; Acrodisc). Open solutions of nanowires were kept in an environment that was cleaned to minimize the presence of dust and all dispersions were analyzed immediately after placement into the rinsed glassware. These solutions were capped with a rinsed watch glass upon completion of each study.

Nanowires dispersed in hexanes are contained in glass or plastic vials for small scale assemblies (*e.g.*, over distances up to 1 cm). This assembly can be driven by the accumulation of charge on the exterior of the vials from a Zerostat antistatic gun (product number: Z108812-1EA; Sigma-Aldrich) held next to the vial. Alternatively, similar assemblies of nanowires can be achieved using a high voltage power supply (Spellman High Voltage DC Supply; with an operating range of 0.1−30 kV) that is connected by copper or platinum wire leads attached to the exterior of the vial. Larger scale assemblies were performed with dispersions of nanowires contained in a glass Petri dish that was suspended in air with either a single clamp or hollow glass supports. The electrodes used for these assemblies were either copper or platinum wires (~1 mm in diameter, 2 to 3 cm in length; ≥99.9%; Sigma-Aldrich) or a stainless steel mesh with open circular holes (Small Parts Inc.). The high voltage power supply is connected to these electrodes *after* positioning the wire or mesh within the suspension of nanowires. *WARNING: use extreme caution when working with high voltages. The system under study should be appropriately grounded, and the working and ground electrodes should be at least 3 cm apart while performing the electrokinetic assembly to avoid arcing. Sparks created from electrode arcing can easily initiate combustion of the hexanes.* Extreme care should be taken when performing large scale assembly of nanowires in an open dish of hexanes.

Modeling of Electric Field Lines. Simulated spatial distributions of the electric field lines and gradients were performed with COMSOL Multiphysics 3.5 using the constitutive relation, $D = \varepsilon_0 \times \varepsilon_r \times E$ for two spherical electrodes immersed in water contained within a glass Petri dish. Water was used as the solvent for this simulation as we were not able to model highly insulating solutions, such as hexane. Scaling for this simulation was identical to that for the experimental conditions. The two opposing spherical electrodes (each with a radius of 0.65 cm) were spaced 4.6 cm apart (center-to-center distance) within the glass Petri dish. This dish had a volume of $\pi r^2 h$, where $r = 4.25$ cm and $h = 1.3$ cm. Physical properties of water (at a temperature of 293 K) entered into the model include relative permittivity, $\varepsilon_r = 1$; conductivity, $\sigma = 5.5 \times 10^{-6}$ S/m; and viscosity, $\eta = 1.003$ mPa·s. In addition, potentials of −5000 and +5000 V under DC conditions were applied to the working and ground electrodes, respectively.

Acknowledgment. This research was supported in part by the Natural Sciences and Engineering Research Council (NSERC) of Canada, the Canada Research Chairs Program, the France-Canada Research Fund, and Simon Fraser University (Trust Endowment Fund). This work made use of 4D LABS shared facilities supported by the Canada Foundation for Innovation (CFI), British Columbia Knowledge Development Fund (BCKDF), Western Economic Diversification Canada, and Simon Fraser University. The authors also thank Jeff Rudd from the Physics Department at Simon Fraser University for providing the high voltage power supply for this research.

Supporting Information Available: Electron microscopy, X-ray photoelectron spectroscopy, and X-ray diffraction data are provided for both selenium and silver nanowires used in these studies. In addition, further data is provided on the electrokinetic assembly of these semiconducting and metallic nanowires to form macroscopic fibers under applied electric fields. This data includes analysis on stability of these assemblies. COMSOL modeling of the electric field lines between two spherical electrodes is simulated by a finite element method, and data is included to compare these field lines to the organization of fibers assembled from nanowires. This material is available free of charge *via* the Internet at http://pubs.acs.org.

REFERENCES AND NOTES

1. Lu, X. M.; Rycenga, M.; Skrabalak, S. E.; Wiley, B.; Xia, Y. N. Chemical Synthesis of Novel Plasmonic Nanoparticles. *Annu. Rev. Phys. Chem.* **2009**, *60*, 167–192.

2. Hu, J. Q.; Bando, Y.; Golberg, D. Novel Semiconducting Nanowire Heterostructures: Synthesis, Properties and Applications. *J. Mater. Chem.* **2009**, *19*, 330–343.
3. Kuno, M. An Overview of Solution-Based Semiconductor Nanowires: Synthesis and Optical Studies. *Phys. Chem. Chem. Phys.* **2008**, *10*, 620–639.
4. Zhang, W. X.; Yang, S. H. In Situ Fabrication of Inorganic Nanowire Arrays Grown From and Aligned on Metal Substrates. *Acc. Chem. Res.* **2009**, *42*, 1617–1627.
5. Andrews, R.; Jacques, D.; Qian, D. L.; Rantell, T. Multiwall Carbon Nanotubes: Synthesis and Application. *Acc. Chem. Res.* **2002**, *35*, 1008–1017.
6. Dai, H. J. Carbon Nanotubes: Synthesis, Integration, and Properties. *Acc. Chem. Res.* **2002**, *35*, 1035–1044.
7. Xia, Y. N.; Yang, P. D.; Sun, Y. G.; Wu, Y. Y.; Mayers, B.; Gates, B.; Yin, Y. D.; Kim, F.; Yan, Y. Q. One-Dimensional Nanostructures: Synthesis, Characterization, and Applications. *Adv. Mater.* **2003**, *15*, 353–389.
8. Hermanson, K. D.; Lumsdon, S. O.; Williams, J. P.; Kaler, E. W.; Velev, O. D. Dielectrophoretic Assembly of Electrically Functional Microwires from Nanoparticle Suspensions. *Science* **2001**, *294*, 1082–1086.
9. Koh, S. J. Strategies for Controlled Placement of Nanoscale Building Blocks. *Nanoscale Res. Lett.* **2007**, *2*, 519–545.
10. Hong, S.; Kim, T. H.; Lee, J.; Byun, K. E.; Koh, J.; Kim, T.; Myung, S. "Surface-Programmed Assembly" of Nanotube/Nanowire-Based Integrated Devices. *Nano* **2007**, *2*, 333–350.
11. Heo, K.; Kim, C. J.; Jo, M. H.; Hong, S. Massive Integration of Inorganic Nanowire-Based Structures on Solid Substrates for Device Applications. *J. Mater. Chem.* **2009**, *19*, 901–908.
12. Lu, W.; Lieber, C. M. Nanoelectronics From the Bottom Up. *Nat. Mater.* **2007**, *6*, 841–850.
13. Tao, A. R.; Huang, J. X.; Yang, P. D. Langmuir-Blodgettry of Nanocrystals and Nanowires. *Acc. Chem. Res.* **2008**, *41*, 1662–1673.
14. Acharya, S.; Hill, J. P.; Ariga, K. Soft Langmuir-Blodgett Technique for Hard Nanomaterials. *Adv. Mater.* **2009**, *21*, 2959–2981.
15. Mastrangeli, M.; Abbasi, S.; Varel, C.; Van Hoof, C.; Celis, J. P.; Bohringer, K. F. Self-Assembly from Milli-to Nanoscales: Methods and Applications. *J. Micromech. Microeng.* **2009**, *19*, 083001.
16. Fan, Z. Y.; Ho, J. C.; Takahashi, T.; Yerushalmi, R.; Takei, K.; Ford, A. C.; Chueh, Y. L.; Javey, A. Toward the Development of Printable Nanowire Electronics and Sensors. *Adv. Mater.* **2009**, *21*, 3730–3743.
17. Lu, W.; Lieber, C. M. Semiconductor Nanowires. *J. Phys. D: Appl. Phys.* **2006**, *39*, R387–R406.
18. Wang, M. C. P.; Gates, B. D. Directed Assembly of Nanowires. *Mater. Today* **2009**, *12*, 34–43.
19. Zhang, Y. G.; Chang, A. L.; Cao, J.; Wang, Q.; Kim, W.; Li, Y. M.; Morris, N.; Yenilmez, E.; Kong, J.; Dai, H. J. Electric-Field-Directed Growth of Aligned Single-Walled Carbon Nanotubes. *Appl. Phys. Lett.* **2001**, *79*, 3155–3157.
20. Kamat, P. V.; Thomas, K. G.; Barazzouk, S.; Girishkumar, G.; Vinodgopal, K.; Meisel, D. Self-Assembled Linear Bundles of Single Wall Carbon Nanotubes and their Alignment and Deposition as a Film in a dc Field. *J. Am. Chem. Soc.* **2004**, *126*, 10757–10762.
21. Yu, G. H.; Cao, A. Y.; Lieber, C. M. Large-Area Blown Bubble Films of Aligned Nanowires and Carbon Nanotubes. *Nat. Nanotechnol.* **2007**, *2*, 372–377.
22. An, L. B.; Cheam, D. D.; Friedrich, C. R. Controlled Dielectrophoretic Assembly of Multiwalled Carbon Nanotubes. *J. Phys. Chem. C* **2009**, *113*, 37–39.
23. Annamalai, R.; West, J. D.; Luscher, A.; Subramaniam, V. V. Electrophoretic Drawing of Continuous Fibers of Single-Walled Carbon Nanotubes. *J. Appl. Phys.* **2005**, *98*, 114307.
24. Huang, Y. Y.; Knowles, T. P. J.; Terentjev, E. M. Strength of Nanotubes, Filaments, and Nanowires From Sonication-Induced Scission. *Adv. Mater.* **2009**, *21*, 3945–3948.
25. Vijayaraghavan, A.; Blatt, S.; Weissenberger, D.; Oron-Carl, M.; Hennrich, F.; Gerthsen, D.; Hahn, H.; Krupke, R. Ultra-Large-Scale Directed Assembly of Single-Walled Carbon Nanotube Devices. *Nano Lett.* **2007**, *7*, 1556–1560.
26. Zhou, R. H.; Chang, H. C.; Protasenko, V.; Kuno, M.; Singh, A. K.; Jena, D.; Xing, H. CdSe Nanowires with Illumination-Enhanced Conductivity: Induced Dipoles, Dielectrophoretic Assembly, and Field-Sensitive Emission. *J. Appl. Phys.* **2007**, *101*, 073704.
27. Kim, T. H.; Lee, S. Y.; Kim, H. G.; Kim, S. H.; Hong, C. H.; Hahn, Y. B.; Lee, S. K. Characteristics of Dielectrophoretically Aligned UV-blue GaN Nanowire LEDs. *J. Nanosci. Nanotechnol.* **2008**, *8*, 268–273.
28. Boote, J. J.; Evans, S. D. Dielectrophoretic Manipulation and Electrical Characterization of Gold Nanowires. *Nanotechnology* **2005**, *16*, 1500–1505.
29. Lee, J. W.; Moon, K. J.; Ham, M. H.; Myoung, J. M. Dielectrophoretic Assembly of GaN Nanowires for UV Sensor Applications. *Solid State Commun.* **2008**, *148*, 194–198.
30. Smith, P. A.; Nordquist, C. D.; Jackson, T. N.; Mayer, T. S.; Martin, B. R.; Mbindyo, J.; Mallouk, T. E. Electric-Field Assisted Assembly and Alignment of Metallic Nanowires. *Appl. Phys. Lett.* **2000**, *77*, 1399–1401.
31. Besra, L.; Liu, M. A Review on Fundamentals and Applications of Electrophoretic Deposition (EPD). *Prog. Mater. Sci.* **2007**, *52*, 1–61.
32. Velev, O. D.; Bhatt, K. H. On-Chip Micromanipulation and Assembly of Colloidal Particles by Electric Fields. *Soft Matter* **2006**, *2*, 738–750.
33. Pohl, H. A. The Motion and Precipitation of Suspensoids in Divergent Electric Fields. *J. Appl. Phys.* **1951**, *22*, 869–871.
34. Pohl, H. A. Some Effects of Nonuniform Fields on Dielectrics. *J. Appl. Phys.* **1958**, *29*, 1182–1188.
35. Wiles, J. A.; Grzybowski, B. A.; Winkleman, A.; Whitesides, G. M. A Tool for Studying Contact Electrification in Systems Comprising Metals and Insulating Polymers. *Anal. Chem.* **2003**, *75*, 4859–4867.
36. Sakata, S.; Okada, T. Effect of Humidity on Hydrated Cluster-Ion Formation in a Clean Room Corona Discharge Neutralizer. *J. Aerosol Sci.* **1994**, *25*, 879–893.
37. Skoog, D. A.; Holler, F. J.; Nieman, T. A., High-Performance Liquid Chromatography. *Principles of Instrumental Analysis*, 5th ed.; Harcourt Brace & Company: FL, 1998; pp 743.
38. Wohlfarth, C., Permittivity (Dielectric Constant) of Liquids. In *CRC Handbook of Chemistry and Physics*, 90th ed.; Lide, D. R., Haynes, W. M., Eds.; Taylor and Francis: New York, 2009; pp 148−169.
39. Edwards, W. D. High Values for the Electrical Breakdown Strength of Liquids. *J. Chem. Phys.* **1952**, *20*, 753–754.
40. Liao, Z. M.; Hou, C.; Zhao, Q.; Liu, L. P.; Yu, D. P. Gate Tunable Photoconductivity of p-Channel Se Nanowire Field Effect Transistors. *Appl. Phys. Lett.* **2009**, *95*, 093104.
41. Dayeh, S. A. Electron Transport in Indium Arsenide Nanowires. *Semicond. Sci. Technol.* **2010**, *25*, 024004.
42. Talin, A. A.; Leonard, F.; Katzenmeyer, A. M.; Swartzentruber, B. S.; Picraux, S. T.; Toimil-Molares, M. E.; Cederberg, J. G.; Wang, X.; Hersee, S. D.; Rishinaramangalum, A. Transport Characterization in Nanowires using an Electrical Nanoprobe. *Semicond. Sci. Technol.* **2010**, *25*, 024015.
43. Wang, M. C. P.; Gates, B. D. Stabilizing Dispersions of Large Quantities of Selenium Nanowires. *MRS Symp. Proc.* **2008**, *1144*, 1144-LL18-22.
44. Majidi, E.; Gates, B. D. Optimizing the Growth Rates and Thermal Stability of Silver Nanowires. *MRS Symp. Proc.* **2007**, *1017*, 1017-DD18-12.